Simultaneous force and conduction measurements in atomic force microscopy

M. A. Lantz, S. J. O'Shea, and M. E. Welland

Engineering Department, Cambridge University, Cambridge CB2 1PZ, United Kingdom

We used an ultrahigh-vacuum atomic force microscope (AFM) to measure lateral forces and conductivity simultaneously as a function of the applied normal force for nanometer-sized elastic contacts. Metal-coated or bare Si AFM tips are used on cleaved $NbSe_2$ or graphite surfaces. Results are used to compare various means of obtaining the tip-sample contact area (A_0). We find that simple continuum models can give a reasonable description of the mechanical behavior of the contact. Specifically, the Maugis-Dugdale model [D. Maugis, J. Colloid Interface Sci. **150**, 243 (1992)] provides a good basis for describing the elastic contact between an AFM tip and a smooth sample. The theoretical *variation* in contact radius with load is in good agreement with the experimental variation in friction force, conductivity, and lateral tip-sample contact stiffness. To find the contact area A_0, the best approaches appear to be either to fit the applied force data to an appropriate continuum model (provided the contact is elastic) or to measure the lateral tip-sample contact stiffness. In principle we show that conduction AFM methods can be used to find A_0 for Ohmic contacts. However, the uncertainty in the conduction properties of available AFM tips means that at present the absolute value of A_0 cannot be found with confidence. In this regard the use of metal-coated tips can often be misleading for conduction and mechanical measurements because metal wears rapidly off all or some of the tip apex. [S0163-1829(97)07347-5]

I. INTRODUCTION

Engineering surfaces are rough, even at the molecular scale, and when two surfaces are brought together physical contact occurs at a limited number of protruding microscopic asperities. The real area of contact is much smaller than the apparent geometric contact area. A familiar example is that of dry sliding,[1] where the frictional forces acting are dictated by the interaction of the asperities. Thus it has long been recognized that understanding the mechanical behavior of single asperity contacts is essential to understanding fundamental problems of friction, wear, adhesion, and surface deformation.[2] In early experimental studies of microasperities,[3] point contacts were formed under applied loads of μN or more and contact diameters were greater than ~ 30 nm. Recent experimental advances based on scanning probe microscopy (SPM), such as scanning tunneling microscopy (STM) and atomic force microscopy (AFM), offer an alternative means of studying single asperity contacts. Using SPM techniques one can investigate contacts at very low loads ($\ll 1$ nN) and with atomic scale contact area. An additional advantage of SPM methods is that one can simultaneously obtain topographic information of the surface being studied.

Important pioneering work in the use of SPM to study the micromechanics of point contacts was performed by Dürig and co-workers,[4] who used STM to investigate the adhesion, yield strengths, and plastic deformation of metal-metal contacts at the atomic scale. Since only current is measured directly in STM, the forces acting at the tip-sample contact are measured by mounting the sample on a compliant cantilever, and monitoring the deflection of the lever. A much studied corollary of this work is to use the atomic scale junctions formed at the metal contact to study current transport through one-dimensional structures.[5]

In comparison to STM, lateral and normal forces can be measured directly using AFM.[6,7] The ability to measure frictional forces acting at the junction is particularly significant for tribology applications, and in this regard the assertion that the AFM tip-sample contact can behave as a single asperity has been experimentally verified.[8] The techniques and issues involved in the experimental determination of both normal and tangential forces are now understood. However, a difficult and general problem in AFM is to determine the effective area of tip-sample contact (A_0). Such a measurement is necessary to obtain quantitative micromechanical information, such as pressures and shear strengths, at the tip-sample junction. These are parameters of considerable importance in understanding the mechanics of the contact. For example, at what pressure does plastic deformation commence? In friction experiments, at what applied pressure or shear does a boundary lubricant fail? Also note that direct knowledge of A_0 enables a clearer interpretation of the physical basis of obtaining topographic AFM images.

In a previous study,[9] the friction forces and lateral stiffness acting at an AFM contact were measured, and shown to be self-consistent with the Maugis-Dugdale model[10] of the contact mechanics. The consistency of the results suggested that a reasonable estimate of A_0 can be found by either modeling the elastic behavior of the contact as a function of the measured normal force, or by using the measured lateral contact stiffness. In this paper we further investigate the problem of determining the AFM contact area by measuring the electrical conduction through the tip-sample contact, which is one of the traditional means of obtaining A_0.[3] Briefly we find that electrical conductivity measurements can give useful information on the changes in the contact area as the normal and lateral forces vary, even for nanometer-sized contacts. However, we could not obtain the absolute value of A_0 with confidence from the conductivity. This is not a gen-

eral problem, but rather is a consequence of the present limitations of the tips used for conduction AFM, i.e., given a mechanically and electrically stable AFM tip with Ohmic electrical characteristics, we believe reliable measurements of A_0 can be made on conducting surfaces.

All the present experiments are performed using commercially available Si AFM tips in contact with atomically smooth, conducting surfaces [highly oriented pyrolytic graphite (HOPG) and NbSe$_2$] under UHV conditions. In principle the methods discussed can be used in more general AFM situations, such as in air or liquids, but the interpretation of such data is necessarily less straightforward. Similarly, for this preliminary study we only consider elastic contacts, and do not investigate the regime of plastic deformation.

II. BACKGROUND

Several methods appear feasible for addressing the problem of finding A_0, and thus obtaining useful micromechanical information. Meyer and co-workers[11] inferred the geometric extent of the contact area from topography images. In our study the following, more general techniques are discussed.

(i) Measurement of applied normal force. Provided A_0 is not so small (~ 1 nm^2) that atomic structure dominates,[4] A_0 can be estimated by an appropriate continuum mechanics equation which relates the applied normal force acting on an asperity to the mechanical contact area. For example, the earliest and simplest model for an elastic contact was given by Hertz[2] for a sphere on a flat. In this case,

$$A_0 = \pi a^2 = \pi (3PR/4E^*)^{2/3} \quad (1)$$

where P is the applied normal force, a is the contact radius, R is the radius of curvature of the tip, and E^* is the combined elastic modulus of the tip and sample. Thus if R and E^* are known, one can infer A_0 by fitting the measured normal force to Eq. (1).

The Hertz theory cannot be used if adhesive forces are present. In such cases more refined approaches are used, which take into account the surface forces acting on the tip. To determine the appropriate continuum model to apply, we note that the ratio of elastic deformation in the contact to the distance over which surface forces act can be expressed by the nondimensional parameter ϕ, given by[3]

$$\phi = \left(\frac{Rw^2}{E^{*2} z_0^3} \right)^{1/3}, \quad (2)$$

where w is the work of adhesion, and z_0 is the equilibrium spacing for the Lennard-Jones potential of the surfaces. For $\phi > 5$ the Johnson-Kendall-Roberts (JKR) theory[12] provides a good model of the contact, whereas for $\phi < 0.1$ the analysis by Bradley[13] or the Derjaguin-Muller-Toporov (DMT) model[14] are more appropriate. In the intermediate regime, the Maugis-Dugdale theory[10] provides an approximate closed-form analysis and this is the model we adopt because for typical AFM operation with sharp tips, $\phi \sim 1$.

In the Maugis-Dugdale model intimate contact (zero separation) between the two surfaces occurs within a circular area of radius a, as illustrated in Fig. 1. The attractive interaction
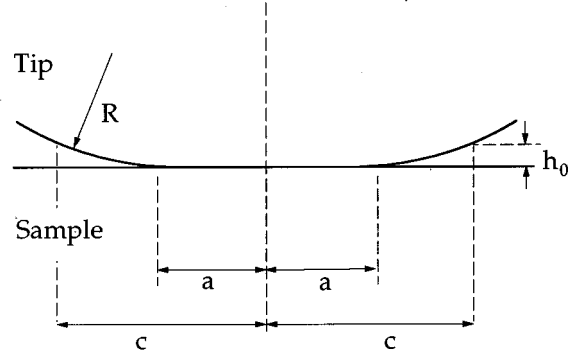

FIG. 1. Maugis-Dugdale model of the tip-sample contact. Intimate contact occurs within a circular region of radius a. A constant attractive force continues to act over a larger circular region of radius c. The attractive force falls to zero at a tip-sample distance h_0 which is typically around 2 Å.

between the surfaces extends over a larger circular region, of radius c. In the region between c and a the surfaces separate slightly by a distance increasing from zero at $r=a$, to h_0 at $r=c$. The adhesive force between the two surfaces is assumed to have a constant value σ_0 until the separation h_0 is reached, at which point the adhesive force falls to zero. The value of h_0 is chosen such that the maximum attractive force and the work of adhesion match those of a Lennard-Jones potential, i.e., $\sigma_0 h_0 = w_{L-J}$, from which one finds $h_0 = 0.971 z_0$. The values of the radii a and c can be found by simultaneously solving two equations containing a, c, and the nondimensional parameters

$$\bar{P} \equiv \frac{P}{\pi w R} \quad \text{and} \quad \lambda = 2\sigma_0 \left(\frac{9R}{16\pi w E^{*2}} \right). \quad (3)$$

It can be shown that $\lambda = 1.16\phi$. The effective radius b, over which lateral forces act, lies somewhere between a and c, i.e., $b = a + n(c-a)$, where $0 < n < 1$. In this work we assume that $n = 0.4$, as this corresponds approximately to the maximum attractive force in the Lennard-Jones interaction. Further details of the model were given by Johnson.[10]

Note that all continuum models require an estimate of E^* and the radius of curvature of the AFM tip. These parameters are difficult to ascertain, and may be subject to considerable uncertainty. In our experiments R is measured using high-resolution electron microscopy,[15,16] and E^* is calculated using bulk material properties. In the Maugis-Dugdale model we must also assume values of z_0 and n.

(ii) Measurement of contact compliance. For the elastic deformation of a point contact one can relate a measured compliance or contact stiffness (k_{contact}) to the radius of the contact area by simple equations of the form

$$k_{\text{contact}} \approx 2E^* a \quad (4)$$

when the tip is displaced in the surface normal direction,[17] or

$$k_{\text{contact}} \approx 8G^* a. \quad (5)$$

when the tip is displaced in the surface lateral direction,[9,18] where G^* is the combined shear modulus of the tip and sample. Therefore, by measuring k_{contact} we can solve for the contact radius using the bulk material properties of the tip

and sample. This has the uncertainty in assigning a value to E^* or G^*, but this difficulty is inherent to all continuum models. In AFM, $k_{contact}$ is measured by applying either a small force or displacement modulation to the junction in the surface normal direction [for Eq. (4)] or in the surface lateral direction [for Eq. (5)] and monitoring the tip response. Details of the experimental techniques are given elsewhere.[9,17,18] We only note that care is required if displacement modulation is used to ensure that all the system compliances have been considered.[16]

(iii) Measurement of conductivity. The conductivity of the tip-sample contact can be measured[1,3] and A_0 found using the relevant current-voltage (I-V) characteristic for the junction, since the current flow is invariably some function of the junction area. Briefly, the I-V characteristic between tip and sample can take on many forms depending on the principle conduction mechanism involved. In conduction AFM the material of the tip apex consists of either pure metal or heavily doped semiconductor. For purely Ohmic contacts (i.e. metal-metal contacts), the I-V is of the typical spreading resistance form

$$R_{spreading} = \frac{\rho}{2a}, \qquad (6)$$

where ρ is the mean resistivity of the tip and sample. This is the traditional method of finding A_0 in point-contact studies, and holds if $L \ll a$, where L is the mean free path of the conduction electrons. Typically $L \sim 100$ Å in metals. In AFM, it is not uncommon for contact areas to be very small, such that $L > a$. In this case the appropriate contact resistance is given by the Sharvin expression

$$R_{Sharvin} = \frac{4\rho L}{3\pi a^2}. \qquad (7)$$

Semiconductor-type point contacts are more difficult to characterize experimentally.[19] In general we cannot obtain an accurate estimate of the absolute value of the contact area because some of the parameters of the complete I-V characteristic are not known. An example of this difficulty is detailed below for a Si tip on NbSe$_2$. Nevertheless, at a *fixed* bias voltage across the junction the current is always proportional to A_0 for any of the current transport mechanisms encountered (e.g. direct tunnelling, thermionic emission, etc.).[20] Therefore it is possible to equate the *variation* in current at a constant bias to variations in contact area.

Finally we note that the friction forces acting on an asperity also depend directly on the contact area, and an important attribute of AFM is that the lateral forces can be measured directly.[6] Details of the many AFM tribology studies and interpretation can be found elsewhere.[21] In this work we only wish to note that for an AFM tip sliding with no wear on a molecularly smooth surface the friction force (F_f) can be related to the contact area by,[1]

$$F_f = \tau A_0, \qquad (8)$$

where τ is the shear strength of the junction. The essential features of this simple description of interfacial sliding have been verified experimentally.[8,22] In this study we measure the variation in F_f as a function of the applied normal force, and

compare Eq. (8) with the values of A_0 expected from methods (i) and (iii) above. We do not consider Eq. (8) as a general means of finding A_0. Rather it is a description of the friction behavior which must be verified for a given interface. The parameter τ is not known *a priori* from bulk measurements and one does not anticipate Eq. (8) to be as simple on rough surfaces where surface topography (e.g., step edges) will give rise to additional lateral forces acting on the tip. Furthermore, variations in surface chemistry may also alter the friction force, irrespective of variations in A_0.

III. RESULTS

A. Experiment

The experiments were performed using an optical deflection-type UHV AFM. The tip-sample distance can be maintained using either constant force AFM or constant-current STM control. Heating and argon ion sputtering are available for cleaning, although in this work the HOPG and NbSe$_2$ samples were never sputtered, as this would roughen the surfaces. The base pressure of the system is 5 $\times 10^{-10}$ Torr.

The basic experimental results consist of force curves and I-V curves. In an I-V curve a linear voltage ramp is applied between the tip and sample, and the resulting current flow measured. A standard STM current to voltage converter is used in this study (adjustable gain 10^7–10^{10} V/A). For high conductivity (e.g., metal-metal) junctions a logarithmic current amplifier is often more useful. The I-V characteristics provide an electrical characterisation of the junction.

To obtain force curves, which characterize the mechanical behavior of the junction, the sample is either retracted from or ramped toward the tip, and the resulting cantilever displacement logged. The applied force acting on the tip is then given by the cantilever spring constant multiplied by the lever displacement. Simultaneously, lateral forces and conduction can be measured. For conduction force curves, a fixed voltage is applied between the tip and sample, and the current is measured as the applied force changes. For lateral force measurements (we measure either the static friction force or the lateral contact stiffness) the twisting of the lever due to a lateral sample displacement is measured.[8,21] Briefly, the sample is displaced using a triangular voltage wave form applied to the piezoelectric scan tube. The resulting lateral force acting on the tip apex exerts a torque which twists the cantilever beam. The twisting of the beam is detected in the optical deflection system using a quadrant position photodetector. Because of the applied periodic sample displacement the lateral component of the photodetector signal is also periodic, the amplitude of which gives a measure of the magnitude of the lateral forces. For the experiments described here, the wave-form amplitude is continuously measured using a lock-in amplifier. A lateral sample oscillation of ~ 100 Å$_{p\text{-}p}$ is used for friction force data, in which the tip slides over the surface, whereas an oscillation of ~ 5 Å$_{p\text{-}p}$ is used for lateral contact stiffness measurements, in which the tip does not slip. Further details can be found in Refs. 8, 9, and 16.
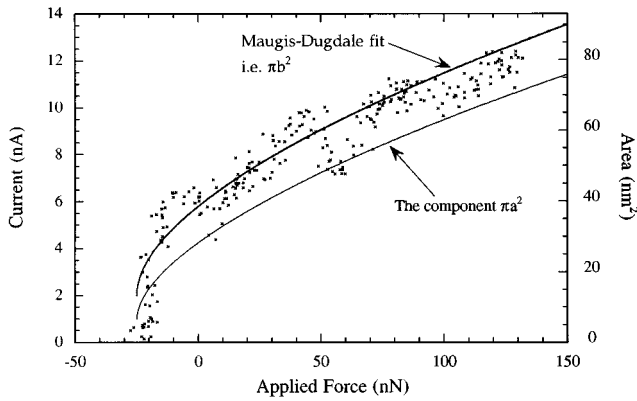
FIG. 2. The current (points) vs applied force for a PtIr-coated Si tip on HOPG. A constant sample bias of 5.6 mV is applied. The solid lines show the Maugis-Dugdale fit to the contact area, with parameters $\lambda = 0.6$ and $b = a + 0.4(c - a)$. The effective Maugis-Dugdale contact area is πb^2. The area πa^2 is that of the intimate contact region.

B. Ohmic contact: Metal coated tip on graphite

The first set of experiments were performed on cleaved HOPG using a silicon cantilever sputter coated with a 20-nm film of 90% platinum/10% iridium. The spring constant of the cantilever in the normal direction was determined to be $k_{normal} = 43$ N/m.[23] Sample preparation consisted of cleaving a HOPG sample immediately prior to transfer into vacuum, and then heating to 400 °C for 1 h prior to the experiments. The tip was cleaned by baking at ~ 130 °C for 12 h, and then Ar^+ sputtering for 3 min (5-kV ions giving $\sim 0.5 - \mu$A target current). To preserve the Pt Ir coating on the tip apex, the STM mode was used for feedback control. Imaging (current set point 1.2 nA, sample bias 60 mV) showed the HOPG surface was characterized by large, atomically flat terraces. The force curves were obtained well away from the terrace edges, and no change in the sample surface was detectable in STM images taken after the experiments. To obtain a force curve the control loop was frozen, the sample bias was reduced to 5.6 mV, and the sample was ramped forward a distance of 45 Å. The sample was then retracted by 75 Å at a rate of ~ 5 Å/s, while the current and cantilever deflection were logged. At the end of the experiment the sample bias was increased back to 60 mV, and feedback control restored.

Approximately 50 force curves were taken at various locations on the sample. A similar variation in current with applied force was observed in each experiment, as shown in Fig. 2. Also shown is the variation in contact area as predicted from the Maugis-Dugdale theory.[10] The agreement between experiment and theory is good, although this is not the case very close to the pull-off force ($P_c = -25$ nN), where we note that the current falls to zero at -21 nN (i.e., before the tip-sample separation at -25 nN). This behavior requires further investigation using noncoated tips, as a distinct possibility is that the metal has worn from an area of radius ~ 1 nm around the tip apex. We find this is a common problem for all metal coated tips (see Sec. III D below for further comments). Nevertheless, the good agreement over the greater part of the force curve implies that (a) the continuum contact mechanics model provides a reasonable description of the contact, and (b) the current flow is a direct measure of the tip-sample contact area, i.e., the current is proportional to A_0. The proportionality implies that Eq. (7) is applicable in this experiment, and that the electron transport is ballistic. We do not expect the spreading resistance term (which is *not* proportional to A_0) to be important since $a < 100$ Å, and indeed Eq. (6) does not give a good fit to the Maugis-Dugdale variation in contact radius.

The agreement between the *variation* in current and the continuum model gives us confidence that A_0 can be found for nanometer sized contact areas using conduction AFM. However, there are technical difficulties we wish to highlight if consistent and reliable values of the *absolute* value of A_0 is required. As an example, consider Fig. 2 for the HOPG/PtIr system. The Maugis-Dugdale model gives the effective contact radius at zero applied force as 3.5 ± 1.4 nm.[24] The conductivity value of the radius at zero applied force is 3.3 ± 1.5 nm, which is found from Eq. (7) using $\rho = 1000 - 5000$ $\mu\Omega$ m,[25] and assuming $L = 100$ Å. The theoretical and conduction values of contact radius appear in agreement, and certainly can provide a reasonable estimate of A_0. We note, however, that the error in the HOPG resistivity is high, and, further, we have not considered the uncertainty in the mean free path nor the effect of regions of metal wearing from the tip. Such uncertainties regarding the electrical nature of the junction are even more pronounced for non-Ohmic junctions (as discussed in Sec. III C below), and we have concluded that it is only for metal-metal contacts that we can at present obtain a ''conduction'' estimate of A_0 with confidence. However, the use of metal-metal contacts in AFM gives rise to two problems. (i) At present, microfabricated AFM tips are coated with a thin film to provide a metallic tip. Such tips are not reliable, as in our experience the metal film always wears rapidly from the tip apex, particularly if lateral forces are present.[26] What is required is a homogeneous tip. (ii) There is strong evidence that metal-metal contacts using a tip radius of $R < \sim 100$ nm invariably involve *plastic* deformation, even at negligible loads.[4,27] Therefore, a study of purely elastic contact behavior may not be feasible.

Another difficulty illustrated by this example is what is meant by the contact area at the nanometer level. As shown in Fig. 1, intimate contact (zero separation) occurs within a circular area with radius a, and in the region between c and a the surfaces separate slightly. The effective radius (b) lies between these two values, i.e., we have chosen $b = a + 0.4(c - a)$. The theoretical value of A_0, which is fitted to the data of Fig. 2, shows how πb^2 varies with load. Also shown for comparison is the intimate contact area πa^2. It is seen that $\sim 80\%$ of the effective area in this example is given by the intimate contact region.

Similarly, we can view the current as having two components: one due to the resistance of the intimate contact, and the other due to tunneling across the region of small separation around the periphery of the contact. One finds for metal-metal contacts that the extended nature of the contact presents no difficulty, as the low resistance ($< \sim 10 k\Omega$) through the zero separation area effectively shorts any tunneling path contribution, i.e., the measured conductivity will correspond to the area πa^2. However, if the contact resistance is high, as in the PtIr-HOPG experiments, or when using semiconductor tips, the peripheral contribution can be significant. This situ-

ation may be even more severe in ambient conditions, since any contaminant liquid meniscus, particularly water, can provide a low-resistance current path of significant area.[26] For the data of Fig. 2 the intimate (πa^2) and peripheral ($\pi c^2 - \pi a^2$) contact areas are approximately equal, so if the resistances across each region are comparable then a significant fraction of the measured current will flow through the peripheral region. The Sharvin resistance of the contact is ~ 1 MΩ, and we associate this with conduction through the area $r = 0$ to $r = a$. For $a < r < c$, where the tunnel barrier has collapsed, the resistance varies between ~ 1 MΩ at $r = a$ to 10–50 MΩ at $r = c \approx 2$ Å, where the tunnel barrier is ~ 0.5 eV.[28] The resistance is sufficiently low over the peripheral area to give a significant current path, and the area over which conduction occurs is expected to be larger than the area of zero separation. However, not knowing the exact geometry of the tip-sample gap or tunnel barrier, we cannot provide a simple relation between the effective conduction and mechanical areas. At present, the experimental errors are at least 50% in the contact radius, which masks any attempt to compare these differences between the effective mechanical and electrical contact areas. Notwithstanding this, from the Maugis-Dugdale theory we calculate that the intimate and peripheral areas can only differ by a factor of ~ 2 in typical AFM applications, because the radii are limited to the case $c/a < 2$.

Finally, note that theoretically the radii a and c scale with load in an essentially identical manner.[10] Therefore, the observation that the variation in current closely matches the theoretical variation with load follows even if the current transport mechanism differs in the intimate and peripheral contact regions.

C. Semiconductor contact: Silicon tip on NbSe$_2$

In Sec. III B, it was shown how conductivity can be measured as a function of applied normal force. In this section we show how similar conductivity measurements can be used to monitor simultaneously the variation in A_0 and friction forces acting on the tip as a function of the applied normal force. This is clearly of importance, as Eq. (8) shows there is a direct dependence of friction on A_0 for a single asperity. Metal-coated tips cannot be reliably used because the metal on the tip apex wears rapidly during contact mode AFM. Hence the cantilever used for lateral force studies is microfabricated from heavily doped ($n+$) single-crystal silicon. Unfortunately, as we outline below, this means that we cannot obtain the absolute value of A_0 using the measured conduction, but can only monitor the relative change in A_0 as the friction force changes.

The normal and lateral direction spring constants of the cantilever used were determined to be $k_{normal} = 1.3$ N/m and $k_{lateral} = 117$ N/m.[23] The resistivity of the silicon is 0.01–0.02 Ω cm, and, as received from the manufacturer, the tip is expected to be covered in a native oxide. This insulating layer was removed by immersing the cantilever in 7:1 buffered oxide etch for 20 s. The cantilever was then rinsed in deionized water, and dried in a stream of dry nitrogen. This produces a hydrogen-terminated, conducting silicon surface which is stable in air for ~ 24 h.[29] Within 30 min of etching, the tip was transferred into the UHV load lock chamber.

Immediately prior to performing the conductivity experiments, the tip was further cleaned by Ar$^+$ sputtering for 3 min (5 kV, ~ 0.5-μA target current). Sample preparation consisted of cleaving a NbSe$_2$ sample immediately prior to transfer into vacuum, and then heating to approximately 120 °C for 30 min before the experiments.

Control was maintained in the contact AFM mode with an applied force of a few nN. Imaging showed that the surface was characterized by large flat terraces with the occasional atomic step. A flat and featureless area, well away from the terrace edges, was chosen as the site for the conductivity and friction force curve experiments. Following the experiments, the area where the experiments were performed was imaged, and no change or damage to the surface was noticeable. In the conductivity experiments described below, a bias of -3 V was applied to the sample. The bias results in an additional applied force due to electrostatic attraction between the tip and sample, but a comparison of data taken with and without a bias indicated that the bias only increased the magnitude of the pull-off force by about 1.2 nN. The same variation in friction force with load was observed with either 0 or -3 V bias, even though the friction and normal force curves changed slightly.

The simultaneous variation in friction and conductivity with applied force was measured at a variety of locations on the sample, and an example of a typical unloading experiment is shown in Fig. 3. The same variation in friction and current with applied force was observed for loading and unloading (approach speed 0.6 nm/s), indicating that the contact was elastic for the range of applied forces investigated. The scales on the current and friction axis have been chosen such that the dependence on applied force can be easily compared. It is clear that the variation in current and friction have a similar dependence on applied force. Since the current at constant bias is expected to vary in direct proportion to the tip-sample contact area, the close agreement between the current and friction data of Fig. 3 provides additional support for the hypothesis that the frictional force for an asperity is directly proportional to the tip-sample contact area [Eq. (8)]. The relation between the friction, current, and tip-sample contact area can be investigated further by comparing experiment to the Maugis-Dugdale theory. In order to compare the theory with the friction data, the frictional force is assumed to be proportional to the tip-sample contact area, i.e., $F_{friction} = \tau A_0 = \tau \pi b^2$, where b is the effective contact radius. The validity of the assumption is shown in Fig. 3 by the good agreement between both the friction and current data and the Maugis-Dugdale fit. Note that, for this comparison, we simply scaled the Maugis-Dugdale fit to match the experiment at one point on the force curves (at $P \sim 0$ nN).

Figure 3 shows that conductivity measurements can be used to monitor the variation in A_0 during friction AFM measurements. However, to obtain an absolute value of the area from the current is particularly difficult using semiconductor tips. To illustrate this, consider Fig. 4 which shows the result of a typical I-V experiment performed at an applied force of 1 nN. The I-V is nonlinear, as expected for a metal-semiconductor junction, and for this system the dominant current transport mechanism appears to be thermionic
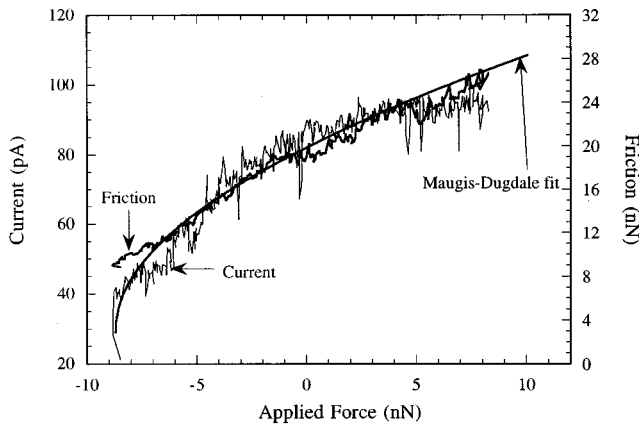
FIG. 3. The variation in current and friction vs applied force for a silicon tip sliding on NbSe$_2$. The lateral sample displacement is 100 Å$_{p\text{-}p}$, and the sample bias is -3 V. The solid line shows the Maugis-Dugdale fit to the contact area, with parameters $\lambda = 0.2$ and $b = a + 0.4(c - a)$.

emission over the junction potential barrier. Therefore, taking the simplest possible case for a Schottky junction, we have[20]

$$I = A_0 J_s (e^{qV/k_B T} - 1), \tag{9}$$

where $J_s = A^* T^2 e^{-q\phi_B/k_B T}$ is the saturation current density, T is the temperature, A^* is the effective Richardson constant, k_B is the Boltzmann constant, q is the elemental charge, and ϕ_B is the barrier height. An extrapolation of a log-linear plot of the forward-bias I-V curve to $V = 0$ gives $(A_0 J_s)$. However to proceed and extract the area A_0, a value of ϕ_B is required, and this is not known with confidence, nor is it possible to calculate J_s from the material properties of the tip and sample, i.e., the exact surface chemistry and doping of the tip apex are uncertain. We find $\phi_B \sim 0.45$ eV for the data of Fig. 4, using the contact area as found from the Maugis-Dugdale theory.

We also studied the lateral contact stiffness (k_{contact}) for a Si tip on a NbSe$_2$ system. This was discussed fully in our previous work.[9] Briefly, we find that the variation with the load of k_{contact} is again very well modeled by the Maugis-
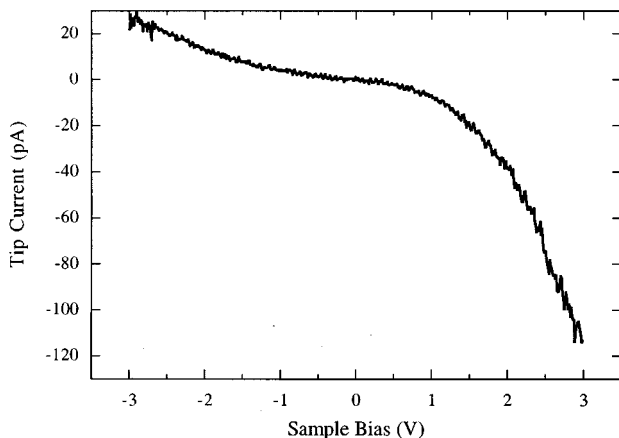

FIG. 4. Current-voltage characteristic of a clean Si tip on NbSe$_2$ at an applied force of $+1$ nN.

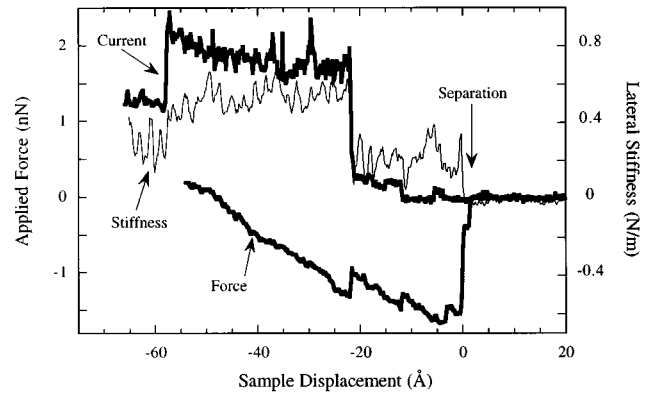

FIG. 5. A force curve showing current, lateral stiffness, and applied force for a clean Si tip on NbSe$_2$. The lever spring constant is $k_{\text{normal}} = 0.5$ N/m. The tip is retracted from the surface, and the displacement is defined as zero at the point where the tip and sample separate. Negative values of displacement correspond to the tip being in contact with the surface. The current is arbitrarily scaled for easy comparison with the stiffness. The sample bias is -3 V, and typical currents are ~ 10 pA. For clarity the applied force is not shown for displacements less than -55 Å.

Dugdale theory. This suggests that Eq. (5) can provide a reasonably simple means of estimating the contact radius using the measured value of k_{contact} and G^*, and indeed the absolute value of A_0 found using the contact stiffness method is in agreement with the calculated Maugis-Dugdale value. For example, for the data of Fig. 3 at zero applied force we find $b = 3.2$ nm from the Maugis-Dugdale theory,[30] and $b = 2.5 \pm 1.2$ nm from contact stiffness experiments using $G^* = 7.0$ GPa. The contact stiffness method also appears to be useful for studies in ambient environments and for non-conducting tip-sample systems.[18]

D. Some cautionary remarks

The force curves vary smoothly with load for the results presented thus far, but this is not always the case. Discontinuous changes in the force, due to either the presence of compliant material at the contact or to changes in the local geometry of the junction (arising from local surface or tip roughness), can be observed with particular tips or samples. An example is given in Fig. 5 which shows the variation in applied force, conduction and lateral stiffness for a Si tip on NbSe$_2$. There is a remarkable correlation between the discontinuous jumps in the data, with both the current and stiffness sometimes even increasing as the load is removed. This suggests that the contact radius changes, in a discontinuous manner. In this particular example the stiffness is very low, and we infer that there is probably an additional compliance, perhaps a wear particle, acting at the junction. It is for this reason we do not call the measured stiffness the ``contact stiffness,'' nor attempt to find a value of the contact radius in this case using Eq. (5). Discontinuous changes in the friction force, again most likely arising from abrupt changes in the tip-sample contact area, can also been observed.

The case with metal-coated AFM tips can produce behavior even further removed from the model of an ideal elastic contact. Here simultaneous current and mechanical measurements may be entirely misleading. Unless care is exercised

e.g., by controlling in STM mode as in Sec. III B the metal coating on the tip apex wears rapidly, and one finds either that (i) a narrow insulating gap forms between the metal coating on the tip and the sample, or (ii) metal from the tip may form a strong adhesive junction with the sample and one observes a large increase in friction, adhesion, and conductivity. In our experiments with gold-coated tips on $NbSe_2$, the force curves and $I-V$ curve can show two general types of behavior, either small adhesion, small static friction, and low, nonlinear conductivity [corresponding to case (i) above]; or high adhesion, high friction, and Ohmic conductivity [case (ii)]. The latter case corresponds to the shearing of a gold-$NbSe_2$ junction. Here the metallic contact area may only be a small part of the total contact area, but the strong interfacial energy associated with the metallic junction dominates the measurements. Even if the metal wears, the metal-sample contact may reform during an experiment if the bias voltage or applied force are sufficiently high. This discussion highlights a general finding from our experiments using a variety of AFM tips, namely, that the material of the tip apex must be homogeneous and preferably have Ohmic characteristics for quantitative conduction measurements to be undertaken at the nanometer scale, especially when lateral forces act on the tip.

IV. CONCLUSION

The important conclusions from the above results and our previous work[9] is that continuum mechanics appears to give a reasonable description of elastic contacts as small as one or two nanometers in radius. The Maugis-Dugdale model provides a good basis for describing the elastic contact between an AFM tip and a smooth sample, and the theoretical variation with load in the contact radius is in good agreement with the experimental variation in friction force, conductivity, and contact stiffness. We note that more study is required to verify this statement fully at applied forces close to the pulloff force. To address the important problem of finding the contact area A_0, the best approaches at present appear to be either to fit the force data to an appropriate continuum model, such as the Maugis-Dugdale theory, or to measure the contact stiffness. It is interesting to note that contact stiffness methods can still be applied even if plastic deformations occur, because there is always some elastic part of the deformation from which we can assess A_0.[31] What is not clear is how useful these methods are under less-controlled conditions than UHV when the material properties of the interfaces (E^* or G^*) are uncertain.

The use of conduction methods with metal-coated or semiconductor tips, while extremely useful to verify the variation in A_0 with load, cannot presently be applied with confidence to find the absolute values of A_0. This contrasts with the situation for traditional metal-metal contactstudies, where conduction methods can be used to find A_0 because the current transport mechanism is well understood. This situation is, however, a consequence of the AFM tips available. While not yet a general method, we believe the results presented show that conduction AFM can give a direct measure of A_0 for micromechanical experiments, provided the tip is sufficiently robust and Ohmic. In this regard we note that the use of metal-coated tips can often be misleading because metal wears rapidly off the tip apex. It is therefore desirable to develop sharp, Ohmic, and homogeneous tips for future conduction AFM studies.

ACKNOWLEDGMENTS

[1] F. P. Bowden and D. Tabor, *The Friction and Lubrication of Solids* (Clarendon, Oxford, 1950), Pt. 1.

[2] K. L. Johnson, *Contact Mechanics* (Cambridge University Press, Cambridge, 1985).

[3] M. D. Pashley, J. B. Pethica, and D. Tabor, Wear **100**, 7 (1984).

[4] U. Dürig, O. Züger, and D. W. Pohl, Phys. Rev. Lett. **5**, 349 (1990); A. Stalder and U. Dürig, J. Vac. Sci. Technol. B **14**, 1259 (1996).

[5] J. I. Pascual, J. Méndez, J. Gómez-Herrero, A. M. Baró, N. Garcia, U. Landman, W. D. Luedtke, E. N. Bogarchek, and H.-P. Cheng, Science **267**, 1793 (1995); G. Rubio, N. Agraït, and S. Vieira, Phys. Rev. Lett. **76**, 2302 (1996).

[6] C. M. Mate, G. M. McClelland, R. Erlandsson, and S. Chiang, Phys. Rev. Lett. **59**, 1942 (1987).

[7] N. A. Burnham, R. J. Colton, and H. M. Pollock, J. Vac. Sci. Technol. A **9**, 2548 (1991).

[8] S. J. O'Shea, M. E. Welland, and T. M. H. Wong, Ultramicroscopy **52**, 55 (1993); R. W. Carpick, N. Agraït, D. F. Ogletree, and M. Salmeron, J. Vac. Sci. Technol. B **14**, 1289 (1996).

[9] M. A. Lantz, S. J. O'Shea, M. E. Welland, and K. L. Johnson, Phys. Rev. B **55**, 10 776 (1997).

[10] D. Maugis, J. Colloid Interface Sci. **150**, 243 (1992); K. L. Johnson, Proc. R. Soc. London, Ser. A **453**, 163 (1997).

[11] E. Meyer, R. Lüthi, L. Howald, M. Bammerlin, M. Guggisberg, and H.-J. Güntherodt, J. Vac. Sci. Technol. B **14**, 1285 (1996); R. Lüthi, E. Meyer, M. Bammerlin, L. Howald, H. Haefke, T. Lehmann, C. Loppacher, H.-J. Güntherodt, T. Gyalog, and H. Thomas, *ibid.* **14**, 1280 (1996).

[12] K. L. Johnson, K. Kendall, and A. D. Roberts, Proc. R. Soc. London, Ser. A **324**, 301 (1971).

[13] R. S. Bradley, Philos. Mag. **13**, 853 (1932).

[14] V. M. Muller, B. V. Derjaguin, and Yu. P. Toporov, Colloids Surface **7**, 251 (1983).

[15] U. D. Schwarz, O. Zwörner, P. Köster, and R. Wiesendanger, in *Micro/Nanotribology and its Applications*, Vol. 330 of *NATO Advanced Study Institute, Series E: Applied Sciences*, edited by B. Bhushan (Kluwer, Dordrecht, 1997), p. 233.

[16] M. A. Lantz, S. J. O'Shea, A. C. F. Hoole, and M. E. Welland, Appl. Phys. Lett. **70**, 970 (1997).

[17] J. B. Pethica and W. C. Oliver, Phys. Scr. **T19**, 61 (1987).

[18] R. W. Carpick, D. F. Ogletree, and M. Salmeron, Appl. Phys. Lett. **70**, 1548 (1997).

[19] Ph. Avouris, I. W. Lyo, and Y. Hasegawa, J. Vac. Sci. Technol. A **11**, 1725 (1993); A. P. Sutton (personal communication).

[20] S. M. Sze, *Physics of Semiconductor Devices* (Wiley, New York, 1981).

[21] E. Meyer, R. Lüthi, L. Howald, M. Bammerlin, M. Guggisberg, and H. J. Güntherodt, in *Micro/Nanotribology and its Applications* (Ref. 15), p. 193; O. Marti, J. Colchero, and J. Mlynek, Nanotechnology **1**, 141 (1990); *Proceedings of the Workshop on the Physical and Chemical Mechanisms of Tribology* [Langmuir **12**, 4481–4609 (1996)].

[22] M. L. Gee, P. M. McGuiggan, J. N. Israelachvili, and A. M. Homola, J. Phys. Chem. **93**, 1895 (1990).

[23] Since the levers are rectangular, the normal and lateral spring constants can be calculated from simple formulas (see Ref. 21 above) which use the dimensions of the lever. We measure the lever width, length, and tip height using a scanning electron microscope. It is more difficult to accurately measure the thickness of the lever and therefore we determine the thickness using the measured first resonance frequency of the unloaded cantilever, as described by M. Nonnenmacher, J. Greschner, O. Wolter, and R. Kassing, J. Vac. Sci. Technol. B **9**, 1358 (1991). The errors in both the normal and lateral spring constants are around 10%.

[24] The relevant parameters for the HOPG/PtIr experiment are $R = 20 \pm 10$ nm, $E^* = 30.9$ GPa (calculated from bulk material properties), and the Maugis-Dugdale parameters $\lambda = 0.6 \pm 0.2$ and $z_0 = 0.2$ nm. The average pull off (adhesive) force was $P_c \approx -25 \pm 5$ nN. We assume the error in E^* is not significant.

[25] Electrical conduction in graphite is Ohmic. However, the resistivity is anisotropic, and varies more between samples than is typical of metals. For conduction parallel to the basal planes the resistivity is $\rho_\parallel \approx 2-4$ $\mu\Omega$ m, and for conduction perpendicular to the basal planes (which is the important direction for the Sharvin resistance component) the resistivity is $\rho_\perp \approx 1000-5000$ $\mu\Omega$ m. See G. W. C. Kaye and T. H. Laby, *Tables of Physical and Chemical Constants*, 14th ed. (Longman, Harlow, UK, 1973).

[26] S. J. O'Shea, R. M. Atta, and M. E. Welland, Rev. Sci. Instrum. **66**, 2508 (1995).

[27] J. B. Pethica, in *Ultimate Limits of Fabrication and Measurement*, Vol. 292 of *NATO Advanced Study Institute, Series E: Applied Sciences*, edited by M. E. Welland and J. K. Gimzewski (Kluwer, Dordrecht, 1995), p. 123; A. P. Sutton and J. B. Pethica, J. Phys. Condens. Matter **2**, 5317 (1990).

[28] N. Agraït, J. G. Rodrigo, and S. Vieira, Ultramicroscopy **42**, 177 (1992).

[29] W. J. Kaiser, L. D. Bell, M. H. Hecht, and F. J. Grünthaner, J. Vac. Sci. Technol. A **6**, 519 (1988).

[30] The force required to separate the tip from the sample was approximately constant for the duration of the experiments at $P_c = -8.0$ nN. Using $P_c = -8.0$ nN and the measured tip radius ($R = 34$ nm), the Maugis-Dugdale theory can be used to calculate the work of adhesion, w, and the elasticity parameter λ. Taking the interaction distance to be $z_0 = 0.2$ nm and $E^* = 40.3$ GPa, values of $\lambda = 0.2$ and $w = 0.042$ J/m^2 are found. These values of λ, w, z, E^*, and R can then be used to calculate the contact radii a, b, and c predicted by the Maugis-Dugdale theory. See Ref. 9.

[31] J. Pethica (personal communication).